THE JOURNAL OF BIOLOGICAL CHEMISTRY
Vol. 273, No. 34, Issue of August 21, pp. 21808–21815, 1998
Printed in U.S.A.

Identification of Effector Residues on Photoreceptor G Protein, Transducin*

(Received for publication, April 14, 1998)

Michael Natochin, Alexey E. Granovsky, and Nikolai O. Artemyev‡

From the Department of Physiology and Biophysics, University of Iowa College of Medicine, Iowa City, Iowa 52242

Transducin is a photoreceptor-specific heterotrimeric GTP-binding protein that plays a key role in the vertebrate visual transduction cascade. Here, using scanning site-directed mutagenesis of the chimeric $G\alpha_t/G\alpha_{i1}$ α-subunit ($G\alpha_{t/i}$), we identified $G\alpha_t$ residues critical for interaction with the effector enzyme, rod cGMP phosphodiesterase (PDE). Our evidence suggests that residue Ile^{208} in the switch II region directly interacts with the effector in the active GTP-bound conformation of $G\alpha_t$. Residues Arg^{201}, Arg^{204}, and Trp^{207} are essential for the conformation-dependent $G\alpha_t$/effector interaction either via direct contacts with the inhibitory PDE γ-subunit or by forming an effector-competent conformation through the communication network between switch II and the switch III/α3-helix domain of $G\alpha_t$. Residues His^{244} and Asn^{247} in the α3 helix of $G\alpha_t$ are responsible for the conformation-independent effector-specific interaction. Insertion of these residues rendered the $G\alpha_{t/i}$ chimera with the ability to bind PDE γ-subunit and stimulate PDE activity approaching that of native $G\alpha_t$. Comparative analysis of the interactions of $G\alpha_{t/i}$ mutants with PDE and RGS16 revealed two adjacent but distinct interfaces on transducin. This indicates a possibility for a functional trimeric complex, RGS/Gα/effector, that may play a central role in turn-off mechanisms of G protein signaling systems, particularly in phototransduction.

The visual transduction cascade in vertebrate photoreceptors represents a classical example of a G protein signaling system. In rod photoreceptor cells, light-activated rhodopsin stimulates GTP-GDP exchange on the retinal G protein, transducin, resulting in dissociation of $G\alpha_t GTP$[1] from $G\beta\gamma_t$ and rhodopsin. Liberated $G\alpha_t$ in active GTP-bound conformation stimulates the effector enzyme, cGMP phosphodiesterase (PDE), by displacing the inhibitory γ-subunits (Pγ) from the PDE catalytic core (Pαβ). cGMP hydrolysis by active PDE results in closure of cGMP-gated channels in the plasma membrane (1–3). As in other G protein cascades, the lifetime of a transducin-mediated signal is linked to the intrinsic GTPase activity of $G\alpha_t$. Hydrolysis of GTP converts the $G\alpha_t$ molecule to the inactive GDP-bound conformation allowing release of Pγ for re-inhibition of Pαβ. A member of the RGS family (4–6), RGS9, and perhaps other retina-specific RGS proteins serve as GTPase-activating proteins (GAPs) for transducin (7–9). They target a transitional intermediate conformation of $G\alpha_t$ during GTP hydrolysis to accelerate GTP hydrolysis and expedite the signal termination (8, 10, 11). The Pγ subunit assists RGS9 in its GAP function, thus providing an elegant feedback mechanism for the effector participation in quenching the visual excitation (7).

Recent progress in understanding molecular mechanisms of G protein action has been advanced by solutions of crystal structures of several G protein α-subunits in active GTP-bound, inactive GDP-bound, and transitional, AlF_4^--complexed conformations (12–16). Three regions of Gα subunits called switches I–III change their conformation upon GTP-GDP exchange (13, 16). One or more of these switches is likely to participate in effector interaction. A wealth of biochemical data on G protein interaction with effectors combined with the structural information allowed a detailed mapping of effector surfaces of Gα subunits. The two well characterized G protein/effector systems are $G\alpha_s$/adenylyl cyclase and $G\alpha_t$/PDE. Initially, several potential effector binding sites corresponding to the α2 helix (switch II), the α3 helix/α3-β5 loop, and the α4-β6 loop were identified on $G\alpha_s$ using a scanning mutagenesis approach (17, 18). Similar regions of $G\alpha_t$ were implicated in the effector interaction. A synthetic peptide, $G\alpha_t$-(293–314) corresponding to the α4-β6 region was shown to activate PDE *in vitro* (19, 20). Sites of the chemical cross-linking of the Pγ subunit to $G\alpha_t$ were also localized to within the α4-β6 loop (21, 22). Analysis of the interaction of $G\alpha_t/G\alpha_{i1}$ chimeras with Pγ strongly implicated the $G\alpha_t$ α3 helix with the α3/β5 loop as a major effector binding region in both basal and activated states (23). The study concluded that the α3-β5 region provides for the specificity of the $G\alpha_t$-Pγ interaction. The second composite Pγ binding site is dependent on the active conformation of $G\alpha_t$ and conserved between $G\alpha_t$ and $G\alpha_{i1}$ (23). Two switch regions of $G\alpha_t$, II and III, have been proposed to participate in the interaction with Pγ (12, 24) and might therefore form such a conserved domain. The switch III region contains a cluster of acidic residues that represent a speculative target for the polycationic region of Pγ which is known to interact with $G\alpha_t$. However, mutation of the acidic cluster did not affect the ability of mutant $G\alpha_t$ to stimulate PDE (25). Evidence for the involvement of the switch II region of $G\alpha_t$ in interaction with PDE is based on the inability of the $G\alpha_t$ mutant W207F to activate the enzyme (24). The involvement of the switch II region of Gα subunits in effector recognition has been supported recently by identification of conserved switch II residues in both $G\alpha_i$ and $G\alpha_s$ required for interaction with adenylyl cyclase (26). The role of the

* This work was supported by National Institutes of Health Grant EY-10843 and American Heart Association Grant-in-Aid 9750334N. National Institutes of Health Grant DK-25295 supported the services provided by the Diabetes and Endocrinology Research Center of the University of Iowa. The costs of publication of this article were defrayed in part by the payment of page charges. This article must therefore be hereby marked "*advertisement*" in accordance with 18 U.S.C. Section 1734 solely to indicate this fact.

‡ To whom correspondence should be addressed. Tel.: 319-335-7864; Fax: 319-335-7330; E-mail: nikolai-artemyev@uiowa.edu.

[1] The abbreviations used are: $G\alpha_t$, rod G protein (transducin) α-subunit; PDE, rod outer segment cGMP phosphodiesterase; Pαβ and Pγ, α-, β-, and γ-subunits of PDE; ROS, rod outer segment(s); uROS, urea-stripped ROS membranes; PγBC, Pγ labeled with 3-(bromoacetyl)-7-diethyl aminocoumarin (BC); GTPγS, guanosine 5′-*O*-(3-thiotriphosphate); RGS proteins, regulators of G protein signaling; GAP, GTPase activating protein; PCR, polymerase chain reaction; GST, glutathione *S*-transferase.

switch II domain and the α3-β5 region as major regions for Gα/effector interactions that emerged from biochemical studies has just been confirmed by the crystal structure of $G\alpha_s$ complexed with catalytic domains of adenylyl cyclase (27, 28).

To define roles of the switch II and α3-β5 regions in the $G\alpha_t$/PDE interaction and identify specific residues required for the effector binding we carried out scanning mutational analysis of these regions in the $G\alpha_t/G\alpha_{i1}$ chimera ($G\alpha_{t/i}$) containing $G\alpha_t$ switch II and $G\alpha_{i1}$ α3-β5. Conserved surface-exposed residues of the $G\alpha_{t/i}$ switch II region were replaced by Ala residues to delineate conserved conformation-dependent effector interactions. $G\alpha_{i1}$ residues that are different between $G\alpha_{i1}$ and $G\alpha_t$ within the α3-β5 region of $G\alpha_{t/i}$ were replaced by corresponding $G\alpha_t$ residues to identify effector-specifying residues of $G\alpha_t$.

EXPERIMENTAL PROCEDURES

Preparation of ROS Membranes, $G\alpha_t$GDP, $G\beta\gamma$, and PγBC—Bovine ROS membranes were prepared as described previously (29). Urea-washed ROS membranes (uROS) were prepared according to protocol in Yamanaka *et al.* (30). $G\alpha_t$GDP was prepared and purified by chromatography on Blue Sepharose CL-6B as described in Ref. 31. $G\beta\gamma_t$ was purified according to Kleuss *et al.* (32). PγBC was obtained and purified as described previously (33). The purified proteins were stored in 50% glycerol at −20 °C or without glycerol at −80 °C.

Site-directed Mutagenesis of Chimeric $G\alpha_{t/i}$—Mutagenesis of $G\alpha_{t/i}$ switch II residues was performed using the vector for expression of His_6-tagged $G\alpha_t/G\alpha_{i1}$ chimera 8 ($G\alpha_{t/i}$) as a template for PCR amplifications (23). The R201A, E203A, R204A, K205A, and K206A substitutions were introduced using 5′-primer 1 and 3′-primers 2, 3, 4, 5, and 6, respectively, for PCR amplification (see below). The PCR products were digested with *Nco*I and *Bam*HI and subcloned into the *Nco*I/*Bam*HI digested $pHis_6G\alpha_{t/i}$. The 5′-primer 1 and 3′-primers 7 and 8 were used to obtain the PCR products carrying the I208A and W207F mutations, respectively. The PCR products were blunt-ended with Klenow fragment, digested with *Nco*I, and ligated into $pHis_6G\alpha_{t/i}$. Prior to the ligation $pHis_6G\alpha_{t/i}$ was digested with *Bam*HI, blunt-ended with mung bean nuclease, and then cut with *Nco*I. The E212A and E212N/G213D substitutions were introduced by PCR using 5′-primers 9 and 10, respectively, and a 3′-primer 11. The PCR products were cut with *Bam*HI and *Hin*dIII and subcloned into the *Bam*HI/*Hin*dIII-digested $pHis_6G\alpha_{t/i}$. The Met^{247}-Lys^{248}-Asp^{251} → Leu^{243}-His^{244}-Asn^{247} (LHN), Met^{247} → Leu^{243} (L), Lys^{248} → His^{244} (H), and Asp^{251} → Asn^{247} (N) mutations were encoded by 5′-primers 12, 13, 14, and 15, respectively, and used for PCR with 3′-primer 11. The Lys^{248}-Asp^{251} → His^{244}-Asn^{247} (HN) mutant was generated by PCR with primers 14 and 11 using the LHN template. The PCR products were digested with *Sph*I and *Hin*dIII and inserted into $pHis_6G\alpha_{t/i}$. A silent *Spe*I site was created in $pHis_6G\alpha_{t/i}$ using QuikChange kit (Stratagene). $pHis_6G\alpha_{t/i}$ was a template for PCR reaction using oligonucleotides 16 and 17, and *Pfu* DNA polymerase. The PCR products were treated with *Dpn*I specific for methylated and hemimethylated DNA and then transformed into *E. coli* DH5α. $pHis_6G\alpha_{t/i}$-*Spe*I was used for PCR-directed mutagenesis with 5′-primer 1 and 3′-primers 18 and 19 to generate a triple mutant Asn^{256} -Lys^{257}-Trp^{258} → His^{252}-Arg^{253}-Tyr^{254} (HRY), and a double mutant Thr^{260}-Asp^{261} → Ala^{256}-Thr^{257} (AT), respectively. The PCR products were inserted into $pHis_6G\alpha_{t/i}$-*Spe*I using *Nco*I and *Spe*I restriction sites. The following primers were used to generate mutant $G\alpha_{t/i}$ (the restriction sites are underlined and mutated codons are in bold): **1,** ATCACGC-CATGGGGGCTGGGGCCAGC; **2,** AGCAGTGGATCCA CTT CTT GCG CTC TGA **CGC** CTG CCC; **3,** AGCAGTGGATCCA CTT CTT GCG **CGC** TGA GCG; **4,** AGCAGT GGATCCA CTT CTT **CGC** CTC TGA GCG; **5,** AGCAGTGGATCCA CTT **CGC** GCG CTC TGA GC; **6,** AGCAGTG-GATCCA **CGC** CTT GCG CTC TGA GC; **7, CGC** CCA CTT CTT GCG CTC TGA GCG CTG; **8,** GAT **AAA** CTT CTT GCG CTC TGA GCG CTG C; **9,** AAGT GGATCC AC TGC TTT **GCG** GGC GTG AC; **10,** AAGT GGATCC AC TGC TTT **AAC GAT** GTG ACT GCC; **11,** TCGTCTTCAA-GAATCGATAAGCTT; **12,** TGAACC GCATGC AT GAA AGC **CTG CAC** CTG TTC **AAT** AGC ATA TG; **13,** TGAACC GCATGC AT GAA AGC **CTG** AAG CTG TTC GAT AGC; **14,** TGAACC GCATGC ATGAA AGT ATG **CAC** CTG TTC; **15,** TGAACC GCATGC AT GAA AGC ATG AAG CTG TTC **AAT** AGC ATA TG; **16,** CAAC AAG TGG TTT ACG GAC ACT AGT ATC ATC CTT TTC CTG AAC; **17,** GTT CAG GAA AAG GAT GAT ACT AGT GTC CGT AAA CCA CTT GTTG; **18,** GAT GAT ACT AGT GTC CGT AAA **GTA CCG GTG** GTT ACA TAT GC; **19,** GAT GAT ACT AGT **GGT CGC** AAA CCA CTT GTT G.

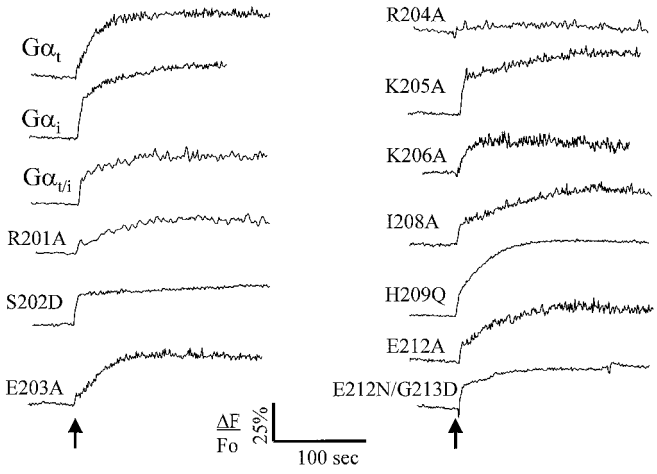

FIG. 1. **Kinetics of AlF_4^--induced increase in the intrinsic tryptophan fluorescence of $G\alpha_t$, $G\alpha_{t/i}$, and its mutants.** Time traces of tryptophan fluorescence of $G\alpha_t$, $G\alpha_{t/i}$, and mutant $G\alpha_{t/i}$ subunits (200 nM) were monitored with excitation at 280 nm and emission at 340 nm. *Arrow* indicates addition of 10 μl of a mixture of $AlCl_3$ and NaF (final concentrations 30 μM and 10 mM, respectively).

The sequences of all mutants were verified by automated DNA sequencing at the University of Iowa DNA Core Facility. $G\alpha_{t/i}$ and all mutants were expressed and purified as described previously (23). The purified proteins were tested in the trypsin protection assay as described previously (34).

Binding of $G\alpha_{t/i}$ and Its Mutants to GST-RGS16—$G\alpha_{t/i}$ or its mutants (1 μM final concentration) were mixed with glutathione-agarose retaining ~10 μg of GST-RGS16 in 200 μl of 20 mM HEPES buffer (pH 7.6), 100 mM NaCl, 4 mM $MgCl_2$ (buffer A) containing 30 μM $AlCl_3$ and 10 mM NaF. After incubation for 20 min at 25 °C, the agarose beads were spun down and washed three times with 1 ml of buffer A, and the bound proteins were eluted with a sample buffer for SDS-PAGE.

Single Turnover GTPase Assay—Single turnover GTPase activity measurements were carried out in suspensions of uROS membranes (5 μM rhodopsin) reconstituted with $G\alpha_{t/i}$ or its mutants (2 μM) and $G\beta\gamma_t$ (1 μM) essentially as described in Refs. 11 and 35. Bleached uROS membranes were mixed with RGS16 (1 μM) and preincubated for 5 min at 25 °C. The GTPase reaction was initiated by addition of 100 nM [γ-^{32}P]GTP (~4 × 10^5 dpm/pmol). The GTPase rate constants were calculated by fitting the experimental data to an exponential function: %GTP hydrolyzed = $100(1 - e^{-kt})$, where k is a rate constant for GTP hydrolysis.

Fluorescence Assays—Fluorescence assays of interaction between $G\alpha_t$ and PγBC were performed on a F-2000 fluorescence spectrophotometer (Hitachi) in 1 ml of buffer A essentially as described in Ref. 33. Where indicated, the buffer A contained 30 μM $AlCl_3$ and 10 mM NaF. Fluorescence of PγBC was monitored with excitation at 445 nm and emission at 495 nm. Concentration of PγBC was determined using ϵ_{445} = 53,000. Time traces of AlF_4^--induced increase in the tryptophan fluorescence of $G\alpha_{t/i}$ and its mutants (200 nM) were recorded on an AB2 fluorescence spectrophotometer (Spectronic Instruments) in a stirred 1-ml cuvette with excitation at 280 nm and emission at 340 nm. Stock solutions of $AlCl_3$ and NaF were mixed immediately prior to injection of 10 μl of the mixture into a cuvette (final concentrations 30 μM $AlCl_3$ and 10 mM NaF).

PDE Activation Assay—HoloPDE was extracted from ROS membranes and purified as described earlier (36). PDE (0.2 nM) was reconstituted with 2 μM $G\alpha_t$GDP or $G\alpha_{t/i}$ mutants and 2 μM $G\beta\gamma_t$ in suspensions of urea-washed ROS membranes containing 10 μM rhodopsin. GTPγS (10 μM) was added to the reaction mixture, and PDE activity was measured using [^{3}H]cGMP similarly as described (37).

Miscellaneous Procedures—Protein concentrations were determined by the method of Bradford (38) using IgG as a standard or using calculated extinction coefficients at 280 nm. SDS-polyacrylamide gel electrophoresis was performed by the method of Laemmli (39) in 12% acrylamide gels. Rhodopsin concentrations were measured using the difference in absorbance at 500 nm between "dark" and bleached ROS preparations. Fitting of the experimental data was performed with nonlinear least squares criteria using GraphPad Prizm (version 2) software. The results are expressed as the mean ± S.E. of triplicate measurements. Examination of the crystal structures of $G\alpha_t$, $G\alpha_i$, and RGS4 was performed using RasMol (version 2.6) software.

TABLE I
Interaction of $G\alpha_{t/i}$ mutants with Pγ and RGS16

	Binding to PγBC		GTPase activity	
	K_d ($G\alpha_{t/i}AlF_4^-$)	K_d ($G\alpha_{t/i}GDP$)	k_{cat}	k_{cat} (+1 μM RGS)
	μM		s^{-1}	
$G\alpha_{t/i}$	0.048 ± 0.004	0.98 ± 0.12	0.015 ± 0.001	0.115 ± 0.017
R201A	1.3 ± 0.1	2.1 ± 0.2	0.018 ± 0.001	0.093 ± 0.008
S202D	0.13 ± 0.01	1.6 ± 0.2	0.014 ± 0.001	0.012 ± 0.001
E203A	0.040 ± 0.004	1.2 ± 0.6	0.010 ± 0.006	0.033 ± 0.002
R204A	1.5 ± 0.1	1.0 ± 0.1	0.012 ± 0.001	0.061 ± 0.005
K205A	0.16 ± 0.03	2.0 ± 0.1	0.022 ± 0.002	0.066 ± 0.004
K206A	0.11 ± 0.02	2.0 ± 0.2	0.010 ± 0.003	0.013 ± 0.04
W207F	3.4 ± 0.3	3.2 ± 0.5	0.012 ± 0.001	0.029 ± 0.003
I208A	3.0 ± 0.2	3.7 ± 0.2	0.023 ± 0.002	0.112 ± 0.014
H209Q	0.073 ± 0.005	2.0 ± 0.3	0.023 ± 0.003	0.102 ± 0.009
E212A	0.038 ± 0.006	1.8 ± 0.2	0.018 ± 0.003	0.133 ± 0.022
E212N/G213D	0.087 ± 0.013	3.1 ± 0.2	0.025 ± 0.001	0.122 ± 0.017
LHN	0.006 ± 0.001	0.035 ± 0.004		
L	0.15 ± 0.01	0.95 ± 0.08		
H	0.026 ± 0.003	0.45 ± 0.06		
N	0.017 ± 0.003	0.34 ± 0.01		
HN	0.008 ± 0.001	0.060 ± 0.002		
HRY	0.20 ± 0.02	1.2 ± 0.1		
AT	0.079 ± 0.007	0.95 ± 0.08		

RESULTS

Expression and Characterization of Mutant $G\alpha_t/G\alpha_{i1}$ Proteins with Substitutions in the $G\alpha_t$ Switch II Region—The following amino acid residues of $G\alpha_t$ switch II that are surface-exposed based on the crystal structure of $G\alpha_tGTP\gamma S$, were selected for the scanning mutagenesis (12): Arg^{201}, Ser^{202}, Arg^{204}, Lys^{205}, Lys^{206}, Trp^{207}, Ile^{208}, His^{209}, Glu^{212}, and Gly^{213}. The surface exposure of Trp^{207} is limited, but this residue had been implicated in the effector interaction previously (24). In addition, we included in our analysis a $G\alpha_t$ mutant E203A as its GDP-bound form was reported to be constitutively active toward PDE (40). Conserved $G\alpha_t$ residues Arg^{201}, Arg^{204}, Lys^{205}, Lys^{206}, and Ile^{208} were replaced by Ala residues. Trp^{207} was substituted by Phe because the $G\alpha_t$ W207F mutant was properly folded when characterized previously (24). Nonhomologous substitutions of the $G\alpha_t$ residues involved in the interactions with RGS proteins, S202D and H209Q, have been generated earlier (41) and utilized in this study. Residues Glu^{212} and Gly^{213} of $G\alpha_t$ are conserved between $G\alpha_t$ and $G\alpha_i$, but $G\alpha_s$ has the Asn-Asp pair instead. Two mutants, E212A and a double mutant E212N/G213D, were made to assess the role of these residues. All mutations of $G\alpha_t$ residues were introduced into $G\alpha_t/G\alpha_{i1}$ chimeric protein, Chi8, which is efficiently expressed in *E. coli*. (23). Chi8 contains more than 80% of the $G\alpha_t$ sequence including all three $G\alpha_t$ switch regions and is fully competent to interact with activated rhodopsin and $G\beta\gamma_t$ (23, 41). For clarity, we refer to Chi8 as $G\alpha_{t/i}$. Expression of $G\alpha_{t/i}$ and all switch II mutants yielded similar amounts of soluble protein (~5 mg/liter of culture).

To critically evaluate the potential role of mutations within the switch II region, it is essential to confirm that these mutations do not interfere with the ability of Gα to undergo conformational change to the active state. Activation of $G\alpha_tGDP$ upon exchange with GTPγS or binding of AlF_4^- leads to an increase in Trp^{207} fluorescence and to protection of the switch II region from cleavage with trypsin (24, 42). Time-traces of AlF_4^--induced tryptophan fluorescence increase for $G\alpha_t$, $G\alpha_{i1}$, $G\alpha_{t/i}$, and the $G\alpha_{t/i}$ switch II mutants are shown in Fig. 1. The fluorescence changes were ~40–45% for $G\alpha_t$, and $G\alpha_{i1}$ and ~35% for $G\alpha_{t/i}$, with similar fast kinetics for $G\alpha_{i1}$ and $G\alpha_{t/i}$, whereas the kinetics for $G\alpha_t$ were slower (Fig. 1). Except for R204A, all $G\alpha_{t/i}$ mutants had comparable (~25–40%) enhancement in tryptophan fluorescence upon addition of AlF_4^-. However, the kinetics of the fluorescence change varied substantially for different mutants from slow, $G\alpha_t$–like, to fast, analogous to $G\alpha_i$. The R204A mutant had a very low degree of fluorescent enhancement (<5%). In the crystal structure of $G\alpha_tGDP{\cdot}AlF_4^-$ ($G\alpha_t{\cdot}AlF_4^-$) side chains of Arg^{204} and Trp^{207} contact one another (15). Perhaps loss of the Arg^{204}/Trp^{207} contact and the Arg^{204}/Glu^{241} salt bridge (43) in the R204A mutant are responsible for the low fluorescence enhancement. Four mutants, R201A, E203A, R204A, and W207F, have displayed a low degree of proteolytic protection (10% or less) in the trypsin protection assay in the presence of AlF_4^- (not shown). Similar reduction in trypsin resistance was observed for analogous mutants of $G\alpha_t$ translated *in vitro* or expressed in COS-7 cells (44). The most stringent criterion for proper folding of $G\alpha_{t/i}$ mutants is the ability to hydrolyze GTP. GTPase activity of $G\alpha_{t/i}$ mutants attests to their ability to interact with $G\beta\gamma_t$ and rhodopsin to exchange GTP for GDP and to undergo activation-inactivation conformational changes. All tested $G\alpha_{t/i}$ switch II mutants had basal GTPase rates ranging from 0.010 s^{-1} to 0.025 s^{-1}, which are comparable to those of $G\alpha_{t/i}$ (0.015 s^{-1}) (Table I) and native $G\alpha_t$ (0.019 s^{-1}) measured under similar conditions (11). Several of the mutated residues, Arg^{201}, Glu^{203}, Lys^{206}, Trp^{207}, and His^{209}, contact $G\beta\gamma_t$ (45), which may account for some variability in observed GTPase rates. A somewhat lower GTPase rate for the E203A mutant is consistent with the catalytic properties of the $G\alpha_i$ E207A mutant (34). Appropriate GTPase activities of R201A, E203A, R204A, and W207F mutants indicate that reduced trypsin protection of these mutants may result from the differences in primary structures rather than distortion of the switch II conformation. Side chains of $G\alpha_t$ Arg^{201}, Arg^{204}, and Trp^{207} may be involved in preventing tryptic cleavage of $G\alpha_t{\cdot}AlF_4^-$ by forming ordered interactions with the switch III/α3 region (13).

Interaction of $G\alpha_{t/i}$ Switch II Mutants with the Pγ Subunit—To identify switch II residues of $G\alpha_t$ essential for effector binding we employed an assay that utilizes the Pγ subunit labeled with the environmentally sensitive fluorescent probe, 3-(bromoacetyl)-7-diethyl aminocoumarin (PγBC) (33). Binding of $G\alpha_tGTP\gamma S$ or $G\alpha_t{\cdot}AlF_4^-$ to PγBC causes ~7-fold maximal increase in the probe fluorescence. Using this assay, affinities of $G\alpha_tGTP\gamma S$ or $G\alpha_t{\cdot}AlF_4^-$ for PγBC are similar (K_d values 2–4 nM), whereas $G\alpha_tGDP$ affinity for PγBC drops by ~20-fold to a K_d of 75 nM (11, 33). Addition of $G\alpha_{t/i}{\cdot}AlF_4^-$ to PγBC led to a maximal fluorescence enhancement F/F_0 of 3-fold. From the binding curve, a K_d for this $G\alpha_{t/i}{\cdot}AlF_4^-/P\gamma BC$ is 48 nM (Fig. 2*A*,

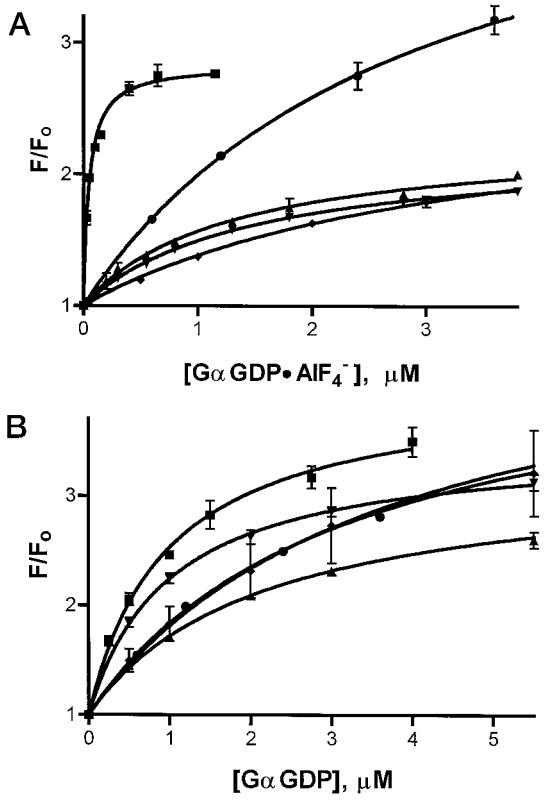

FIG. 2. **Binding of $G\alpha_{t/i}$ and its switch II mutants to PγBC.** The relative increase in fluorescence (F/F_0) of PγBC (10 nM) (excitation at 445 nm, emission at 495 nm) was determined after addition of increasing concentrations of $G\alpha_{t/i}$GDP (■) or its mutants in the presence (*A*) or in the absence (*B*) of AlF_4^-. $G\alpha_{t/i}$ mutants, R201A (▲), R204A (▼), W207F (♦), and I208A (●) that had significantly reduced affinity for PγBC in the presence of AlF_4^-, are shown.

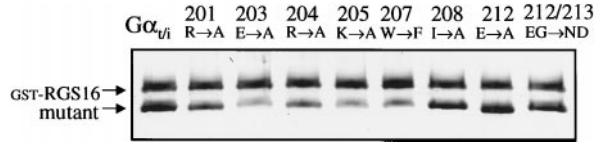

FIG. 3. **Binding of $G\alpha_{t/i}$ switch II mutants to GST-RGS16.** SDS-polyacrylamide gel (12%) stained with Coomassie Blue. Binding of $G\alpha_{t/i}$ and its mutants complexed with GDP and AlF_4^- to GST-RGS16 immobilized on glutathione-agarose was performed as described under "Experimental Procedures."

Table I). As expected, an affinity of $G\alpha_{t/i}$·AlF_4^- for PγBC was lower than that of $G\alpha_t$·AlF_4^-, since in $G\alpha_{t/i}$ the $G\alpha_t$ α3-β5 region is replaced by the $G\alpha_{i1}$ region. The interaction between $G\alpha_{t/i}$ and PγBC was conformation-dependent. The binding curve of $G\alpha_t$GDP to PγBC as measured by the fluorescence increase exhibited a K_d of 0.98 μM and F/F_0 of 4.0 (Fig. 2*B*). Similar relative increases in affinity of $G\alpha_{t/i}$ and $G\alpha_t$ for PγBC upon adoption of an active conformation suggest that $G\alpha_{t/i}$ represents a well suited model protein for mutational analysis to identify residues involved in the GTP-dependent $G\alpha_t$/effector interaction. Four mutants of $G\alpha_{t/i}$ switch II, R201A, R204A, W207F, and I208A in the AlF_4^- conformation had dramatically reduced affinity for PγBC (Table I and Fig. 2*A*). The calculated K_d values for R201A and R204A were 1.3 μM and 1.5 μM, respectively, whereas the K_d values for W207F (3.4 μM) and I208A (3.0 μM) were even higher. Interestingly, the estimated affinities of these four mutants for PγBC did not change significantly in the GDP-bound conformations (Table I, Fig. 2*B*), suggesting that the mutants have lost the conformation-dependent interaction between the $G\alpha_{t/i}$ switch II domain and PγBC. All other $G\alpha_{t/i}$ switch II mutants in both the active and inactive conformations had affinities for PγBC comparable to the respective affinities of $G\alpha_{t/i}$·AlF_4^- or $G\alpha_{t/i}$GDP for the effector protein. Despite a low level of protection in the trypsin sensitivity test, the E203A mutant was fully capable of the conformation-dependent interaction with the effector. Its binding affinity for PγBC was enhanced by ~30-fold in the presence of AlF_4^-, similarly as it was seen for $G\alpha_{t/i}$. These results do not support previously reported constitutive activity of $G\alpha_t$E203AGDP toward PDE (40). Residues Ser^{202}, Glu^{203}, Lys^{205}, Lys^{206}, and His^{209} of $G\alpha_t$ participate in the interaction with RGS proteins based on the crystal structure of RGS4 with $G\alpha_{i1}$·AlF_4^- (46). Substitutions of these residues in $G\alpha_{t/i}$ did not significantly alter its affinity for PγBC (Table I).

Interaction of $G\alpha_{t/i}$ Switch II Mutants with RGS16—The switch II region of Gα subunits is an important domain for binding to RGS proteins (46). To further delineate spatial relationships between the effector and RGS interacting surfaces on $G\alpha_t$, we examined the ability of a human homologue of mouse retina-specific mRGSr (hRGSr or RGS16) (8, 11, 47) to bind the $G\alpha_{t/i}$ switch II mutants and stimulate their GTPase activity. In addition, the competence of $G\alpha_{t/i}$ mutants to interact with RGS may also serve as an indication of the mutant's ability to assume a proper AlF_4^--bound conformation. RGS16 as with most other RGS proteins binds preferentially to the AlF_4^- conformation of G protein α-subunits (8, 10, 11, 48). Binding between the $G\alpha_{t/i}$ switch II mutants and RGS16 was evaluated using precipitation of mutants by glutathione-agarose beads containing immobilized GST-RGS16. The binding assay demonstrated that mutants R201A and R204A had modestly decreased affinity for RGS16, whereas E203A, K205A, and W207F had significant impairment of RGS16 binding (Fig. 3). Two mutants, S202D (41) and K206A (not shown), did not bind to RGS16 using this assay. The binding properties of the mutants correlated well with the capacity of RGS16 to stimulate their GTPase activity in a single turnover GTPase assay (Fig. 4, Table I). GTPase activity of the majority of $G\alpha_{t/i}$ mutants was enhanced by ~4.5–7-fold in the presence of 1 μM RGS16, whereas the response of E203A, K205A, and W207F mutants was notably lower (~2–3-fold) (Fig. 4, Table I). RGS16 failed to stimulate GTPase activity of the $G\alpha_{t/i}$ S202D and K206A mutants (Table I). Explaining our results, side chains of residues Ser^{202}, Glu^{203}, Lys^{205}, and Lys^{206} directly interact with RGS (46). W207F is the only substitution of a non-RGS contact residue that significantly diminished Gα/RGS interaction.

Interaction between $G\alpha_{t/i}$ Mutants with Substitutions within the α3-β5 Region and PγBC—Evidence suggests that the region $G\alpha_t$-(237–270) (the α3 helix and the α3-β5 loop of $G\alpha_t$) participates in a specific interaction between Pγ and both GDP and GTP-bound conformations of transducin (23). Overall structures of $G\alpha_t$ and $G\alpha_i$ including the α3-β5 regions are very similar (12, 14). Therefore, the specificity of $G\alpha_t$ for Pγ within this region is based on the primary structure differences. A limited number of $G\alpha_t$ residues within region $G\alpha_t$-(237–270) are replaced by nonhomologous residues of $G\alpha_i$. Initially we generated the following three mutants of $G\alpha_{t/i}$ in which $G\alpha_{i1}$ residues were substituted by the corresponding $G\alpha_t$ residues: a triple mutant Met^{247}-Lys^{248}-Asp^{251} → Leu^{243}-His^{244}-Asn^{247} (LHN), a triple mutant Asn^{256}-Lys^{257}-Trp^{258} → His^{252}-Arg^{253}-Tyr^{254} (HRY), and a double mutant Thr^{260}-Asp^{261} → Ala^{256}-Thr^{257} (AT). The yields of soluble HRY and AT mutants expressed in *E. coli* were similar to that of $G\alpha_{t/i}$ (~5 mg/liter of culture). Expression levels for the LHN mutant were 4–5-fold lower. However, all three mutants had GTPase activity, trypsin protection, and tryptophan fluorescence enhancement properties similar to $G\alpha_{t/i}$ (not shown). The prediction is that substitutions of the $G\alpha_t$ effector-specific residues for $G\alpha_{i1}$ residues in

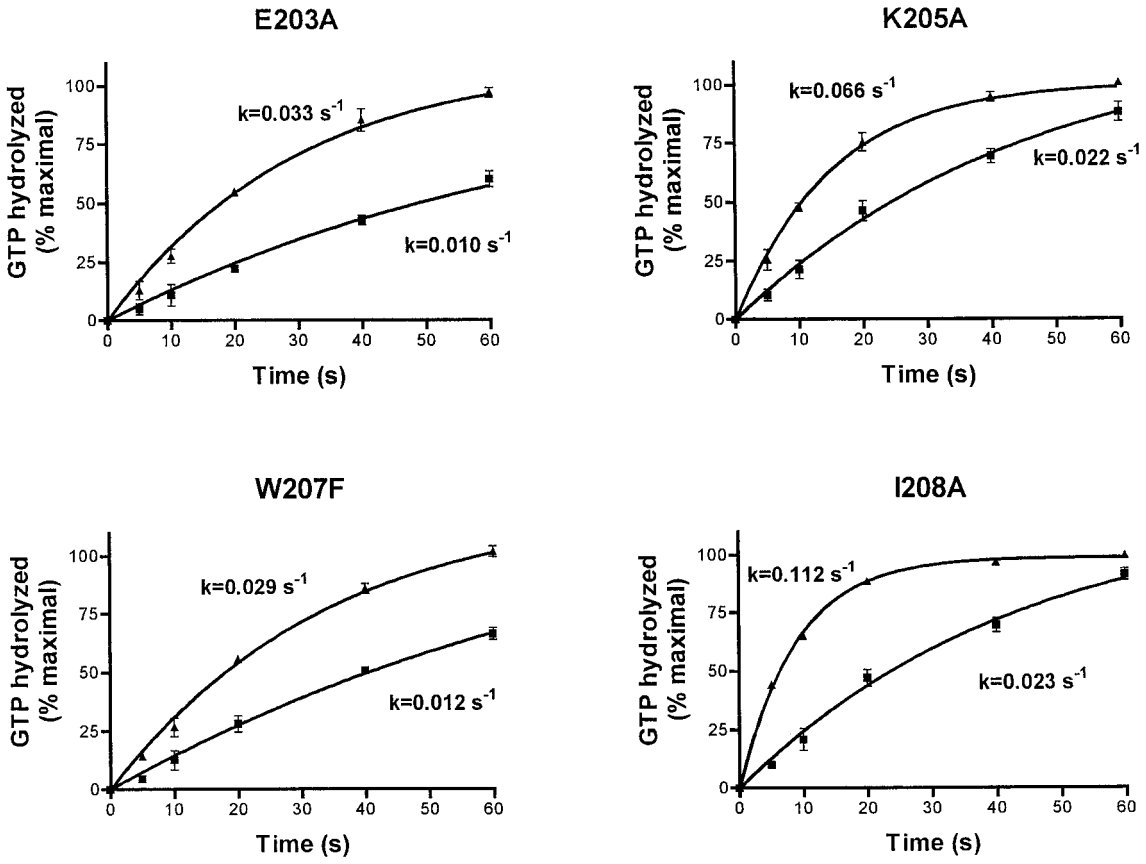

FIG. 4. **Stimulation of GTPase activity of $G\alpha_{t/i}$ switch II mutants by RGS16.** The time course of GTP hydrolysis by selected $G\alpha_{t/i}$ mutants in suspensions of bleached uROS membranes. The reaction mixtures contained 5 μM rhodopsin, 2 μM $G\alpha_{t/i}$ mutant, and 1 μM $G\beta\gamma_t$ in the absence (■) or in the presence (▲) of 1 μM RGS16. The I208A mutant is a representative of $G\alpha_{t/i}$ mutants that have intact GTPase stimulation by RGS16. Mutants E203A, K205A, and W207F had impaired interaction with RGS16.

$G\alpha_{t/i}$ would lead to an increased affinity of such mutant(s) for PγBC. Fig. 5 shows binding of LHN, HRY, and AT mutants in AlF_4^- and GDP-bound conformations to PγBC. The LHN mutant in both AlF_4^- (K_d 6 nM) and GDP-bound (K_d 35 nM) conformations demonstrated a strong increase in affinity for PγBC (Fig. 5, Table I). Furthermore, the K_d value and the larger maximal fluorescence enhancement (F/F_0 ~6-fold) are comparable to those measured for interaction of native $G\alpha_t$ with PγBC (11, 33). Next, we generated three mutants with single substitutions $Met^{247} \rightarrow Leu^{243}$ (L), $Lys^{248} \rightarrow His^{244}$ (H), and $Asp^{251} \rightarrow Asn^{247}$ (N). Expression levels of the L mutant were similar to the yields of the LHN mutant and ~4–5-fold lower then those for the H and N mutants suggesting that Leu^{243} of $G\alpha_t$ is responsible for decreased expression of $G\alpha_t/G\alpha_i$ chimeras containing the $G\alpha_t$-(237–270) segment (23). Mutants H and N in both AlF_4^- and GDP-bound conformations showed improved interaction with PγBC (Fig. 5, Table I). Based on the results obtained with the single substitutions, a double mutant, Lys^{248}-$Asp^{251} \rightarrow His^{244}$-$Asn^{247}$(HN) was made and tested for effector binding. The HN mutation enabled $G\alpha_{t/i}$ to bind PγBC (K_d of 8 nM) with the affinity only ~2-fold lower than that for native $G\alpha_t$ (Fig. 5, Table I).

Activation of Rod HoloPDE by $G\alpha_{t/i}$ Mutants—Binding between $G\alpha_t$ and Pγ represents a simple and informative model assay frequently used to assess the transducin/effector interaction. However, to activate PDE *in vivo* transducin ultimately interacts with Pγ subunits that are not free but complexed with PDE catalytic subunits (1). We tested the ability of $G\alpha_{t/i}$ mutants to stimulate activity of holoPDE reconstituted with urea-washed rod outer segment (uROS) membranes and $G\beta\gamma_t$ in the presence of GTPγS. $G\alpha_{t/i}$ as well as the HRY, AT, and L mutants activated holoPDE very weakly (Fig. 6). Mutants H and N stimulated PDE activity by ~3–4 fold. The triple substitution LHN and the double substitution HN conferred to $G\alpha_{t/i}$ the ability to stimulate basal PDE activity by ~5–6-fold, which was approaching the effects of native $G\alpha_t$ under the same conditions (Fig. 6).

DISCUSSION

Heterotrimeric G protein Gα subunits upon GTP-GDP exchange assume an active GTP-bound conformation that has significantly enhanced affinity for effector proteins. Three regions of Gα subunits undergo the conformational change (switches I-III) and might therefore account for conformation-dependent effector activation (13, 16). Experimental evidence has been accumulated supporting the role of the switch II region of $G\alpha_i$ and $G\alpha_s$ in interaction with adenylyl cyclase. Common and distinct effector residues within switch II regions of $G\alpha_i$ and $G\alpha_s$ have been identified (26). The crystal structure of $G\alpha_s$ complexed with the catalytic domains of adenylyl cyclase has confirmed the $G\alpha_s$ switch II effector-binding residues identified using Ala scanning mutagenesis (27, 28). The data on $G\alpha_t$ switch II participation in effector activation are more limited. The W207F $G\alpha_t$ mutant was shown to have a 100-fold lower affinity for Pγ and was unable to activate PDE (24). The GTPγS-induced conformational change of $G\alpha_t$ brings the exposed side chain of Trp^{207} into contact with the α3 helix (13) and as a result, Trp^{207} is significantly less solvent-exposed in the active conformation of $G\alpha_t$. Therefore, the possibility remained that failure of the W207F mutant to form important contacts with the α3 helix and/or a general distortion of switch II, rather than the loss of the PDE contact residue, is respon-

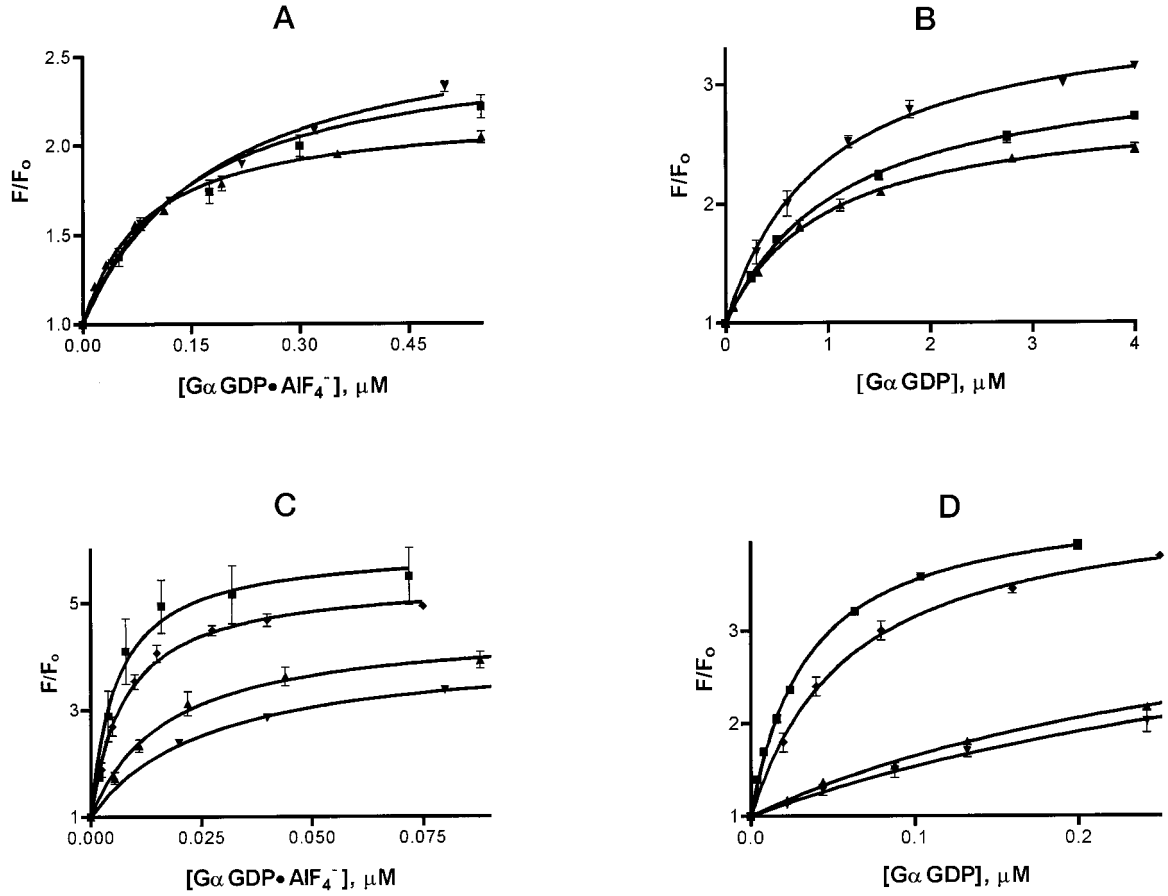

FIG. 5. **Binding of $G\alpha_{t/i}$ α3-β5 mutants to PγBC.** The relative increase in fluorescence (F/F_0) of PγBC (10 nM) (excitation at 445 nm, emission at 495 nm) was determined after addition of increasing concentrations of the following $G\alpha_{t/i}$ mutants. *A* and *B*, HRY (■), AT (▲), L (▼); *C* and *D*, LHN (■), H (▼), N (▲), and HN (♦) in the presence (*A*, *C*) or in the absence (*B*, *D*) of AlF_4^-.

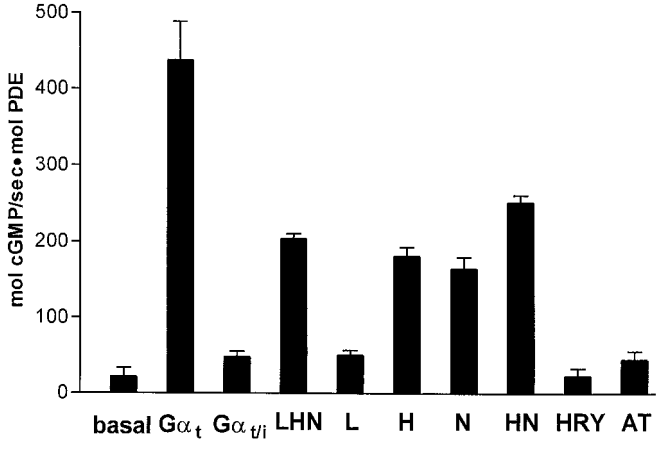

FIG. 6. **Activation of PDE by $G\alpha_t$, $G\alpha_{t/i}$, and $G\alpha_{t/i}$ mutants.** The cGMP hydrolytic activity of rod holoPDE (0.2 nM) was measured in suspensions of urea-washed ROS membranes (10 μM rhodopsin) reconstituted with 2 μM $G\beta\gamma_t$ and 10 μM GTPγS in the absence or presence of 2 μM $G\alpha_t$, $G\alpha_{t/i}$, or $G\alpha_{t/i}$ mutants.

sible for the mutant inability to activate PDE. The recently reported efficient functional expression of $G\alpha_t/G\alpha_{i1}$ chimeric proteins in *E. coli* provided an opportunity for scanning mutational analysis of $G\alpha_t$ residues (23). Our examination revealed four switch II residues, Arg^{201}, Arg^{204}, Trp^{207}, and Ile^{208}, critical for the conformation-dependent interaction between $G\alpha_t$ and Pγ. Most mutations of switch II had very little or no effect on the ability of $G\alpha_{t/i}$GDP to interact with Pγ. However, mutants R201A, R204A, W207F, and I208A in the AlF_4^- conformation had dramatically reduced affinity for PγBC compared with $G\alpha_{t/i}{\cdot}AlF_4^-$. In fact, the affinities of all four mutants for Pγ in the AlF_4^- and GDP-bound forms were similar, suggesting that they lack conformation-dependent interactions with the effector protein.

Do all four residues directly participate in the effector interaction, and how does a single substitution at any of the four positions totally disrupt this interaction? Several scenarios are plausible. Substitution of one of the effector residues could lead to the altered positioning of other residue(s). Side chains of Arg^{204} and Trp^{207} contact each other in the crystal structure of $G\alpha_t{\cdot}AlF_4^-$ (15), and both residues may be reciprocally affected by a single substitution. In addition, the W207F mutation significantly diminished the $G\alpha_{t/i}$/RGS16 interaction, pointing out to a potential distortion of the overall conformation of the mutant switch II region. Finally, and most importantly, the crystal structure of active $G\alpha_t$ shows that side chains of Arg^{201}, Arg^{204}, and Trp^{207} form ordered interactions with residues Glu^{232}, Glu^{241}, Leu^{245}, and Ile^{249} from α3 and switch III (12, 13). Residue Glu^{232} in switch III is critical for coupling switch II to switch III upon $G\alpha_t$ activation (13, 25). The water-mediated contact between Glu^{232} and the guanidino NH group of Arg^{204} (13) might be severed in the R204A mutant. Therefore, residues Arg^{201}, Arg^{204}, and Trp^{207} are crucial for the $G\alpha_t$/effector interaction either by means of direct interaction with Pγ or by forming a communication network between switch II and the switch III/α3 helix domain. In contrast, residue Ile^{208} is well surface-exposed and does not appear to make new GTP-dependent contacts with switches II, III, or the α3 helix. Our data strongly argue in favor of Ile^{208} directly interacting with Pγ in the active conformation of $G\alpha_t$. Comparison of effector residues of $G\alpha_t$, $G\alpha_{i2}$, and $G\alpha_s$ within switch II offers insight

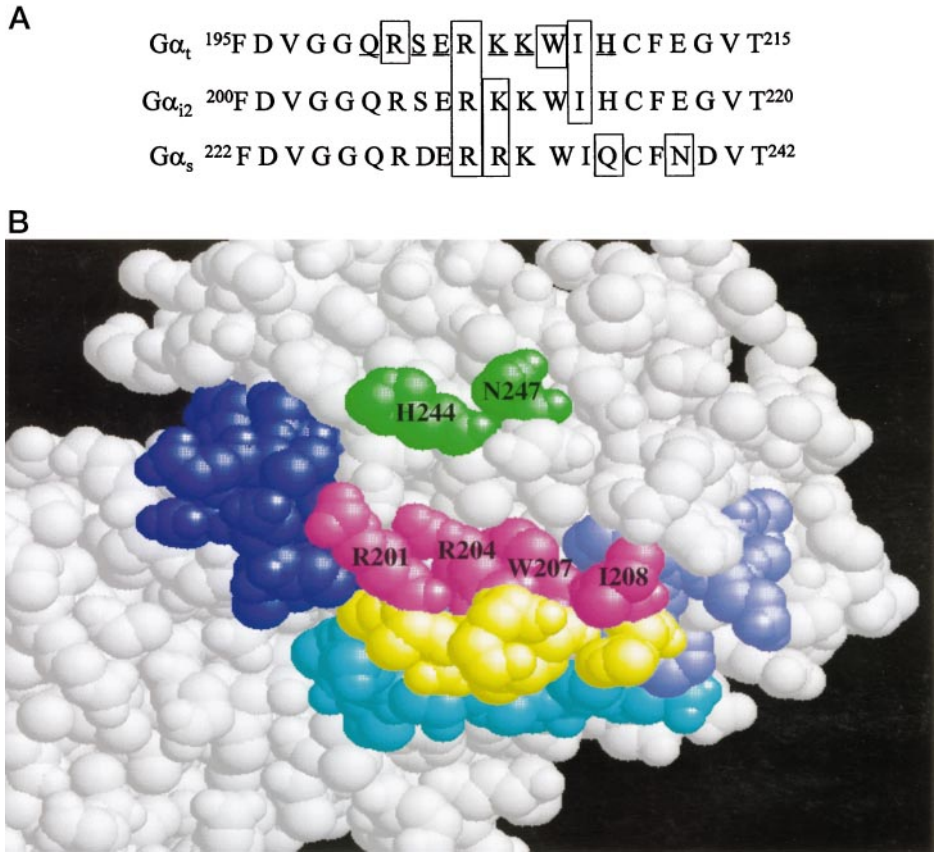

FIG. 7. *A*, effector-interacting residues of Gα subunits. *Boxed* are the residues essential for interacton of $G\alpha_t$, $G\alpha_i$ (26), and $G\alpha_s$ (27, 28) with effectors. *Underlined* are the residues of $G\alpha_t$ that correspond to RGS4-contact residues of $G\alpha_{i1}$ (46). *B*, effector and RGS binding interfaces of $G\alpha_t$. Effector-interacting residues from the switch II region and the α3 helix are shown in *magenta* and *green*, respectively. The $G\alpha_t$ switch II residues corresponding to the RGS4 contacts of $G\alpha_{i1}$ (46) are *yellow*. All other switch II residues are in *light blue*. Switches I and III are shown in *cyan* and *blue*, respectively. The space-filling model was generated using RasMol (version 2.6) software and the coordinates of $G\alpha_t \cdot AlF_4^-$ (15).

into common and individual features of Gα/effector interactions. Although the majority of effector residues are conserved between Gα subunits, distinct conserved residues participate in binding effector molecules. Only the position corresponding to Arg^{204} of $G\alpha_t$ appears to be important in all three Gα subunits (Fig. 7*A*). Arg^{209} in $G\alpha_{i2}$ is the effector residue based on the biochemical evidence (26). Arg^{231} of $G\alpha_s$ makes a backbone contact with adenylyl cyclase (27) (Fig. 7*A*). Ile^{208} in $G\alpha_t$ corresponds to the effector-interacting Ile^{213} in $G\alpha_{i2}$. $G\alpha_s$ exclusively has two non-conserved effector residues, Gln^{236} and Asn^{239} (27, 28). Parallel residues, His^{209} and Glu^{212} of $G\alpha_t$ and His^{214} and Glu^{217} of $G\alpha_{i2}$ are not involved in interactions with effector proteins (Fig. 7*A*).

The conserved switch II region of Gα-subunits is not sufficient to provide specificity to a particular effector among a diverse group of Gα targets. Other Gα regions have been implicated in effector interaction in various G protein signaling systems. The effector role of $G\alpha_s$ α3 helix and α3-β5 loop was reinforced by the crystal structure of the complex between $G\alpha_s$ and catalytic domains of adenylyl cyclase (27). The $G\alpha_t/G\alpha_i$ chimera study provided compelling evidence for the effector-specific conformation-independent interaction domain spanning $G\alpha_t$-(237–270) ($G\alpha_t$ α3 helix and α3-β5 loop) (23). $G\alpha_{t/i}$ utilized in this study represented an excellent tool to map effector residues within this region. Substitutions of the non-conserved $G\alpha_{i1}$ residues by the effector residues of $G\alpha_t$ were expected to produce a "gain-of-function" effect. His^{244} and Asn^{247} of $G\alpha_t$ have been identified as effector-interacting residues. Incorporation of these residues instead of $G\alpha_i$ residues conferred upon $G\alpha_{t/i}$ the Pγ binding potency and ability to stimulate PDE only 2-fold lower than that of native $G\alpha_t$. These residues are located in the α3 helix and are not directly involved in the network of interactions linking α2, α3, and α4 helices of $G\alpha_t$. Most likely, His^{244} and Asn^{247} directly interact with Pγ. Interestingly, His^{244} was one of three residues identified as sites of cross-linking between $G\alpha_t$ and Pγ (22). Also, Asn^{247} aligns with Arg^{256}, which was identified as an effector residue in $G\alpha_q$ (49). Comparison of the α3-β5 effector residues of $G\alpha_t$ and $G\alpha_s$ suggests that two different mechanisms of achieving effector specificity are employed by these Gα subunits (Fig. 7*A*). The effector segment $^{279}NRWLRT^{284}$ of $G\alpha_s$ is relatively conserved with the corresponding $G\alpha_i$ sequence, but it is less homologous to the aligned $G\alpha_t$ segment. The $G\alpha_s$ ability to stimulate adenylyl cyclase is likely due to the shift of its α3-β5 loop from the switch II helix rather than due to the differences in the primary structures of $G\alpha_s$ and $G\alpha_i$ α3-β5 loops (28). Functional properties of the $G\alpha_{t/i}$ HRY and AT mutants indicate that the α3-β5 loop is not involved in the $G\alpha_t$ specific interaction with Pγ. The later interaction is ensured by His^{244} and Asn^{247} in the α3 helix of $G\alpha_t$. Mapping the effector-interacting residues in switch II and α3 regions on the crystal structure of active $G\alpha_t$ shows they are positioned on the same "effector face" of transducin (Fig. 7*B*). The effector interface may also include the α4 helix and α4-β6 loop of $G\alpha_t$ earlier implicated in biochemical studies (19–22, 50). However, an insertion of the $G\alpha_t$-(295–314) segment of $G\alpha_t$ into $G\alpha_{i1}$ only marginally improved the latter's ability to bind Pγ (23). Several residues within the α4-β6 loop of $G\alpha_i$ have been implicated in inhibition of adenylyl cyclase (26). Nonetheless, it is possible that this loop is important for stabilization of the Gα effector interface rather than in direct interactions with effector proteins (28).

In addition to its role as a conformation-sensitive effector binding domain, the switch II region of Gα is also an important site for binding RGS proteins (46). Besides their role as GAPs (48, 51, 52) for the G_i and G_q families, RGS proteins may act as antagonists for some G protein effectors. RGS4 has been shown to block activation of phospholipase Cβ by $G\alpha_q GTP\gamma S$ (53) and to inhibit inositol phosphate synthesis activated by AlF_4^- in COS-7 cells overexpressing G_q (54). However, we demonstrated

earlier that Pγ and RGS16 interact with $G\alpha_t \cdot AlF_4^-$ noncompetitively and that RGS16 acts on the transducin/PDE signaling system to accelerate G protein and effector inactivation rather than to block effector activation (11). The $G\alpha_t$ GAP activity of RGS9, a major photoreceptor RGS protein, has been enhanced by Pγ, supporting simultaneous binding of RGS and Pγ to $G\alpha_t$ (7). To gain more information on spatial relationships between RGS and Pγ binding surfaces on $G\alpha_t$, all $G\alpha_{t/i}$ switch II mutants were examined for their ability to interact with RGS16. Most of the $G\alpha_t$ mutations that impaired interaction with RGS16 coincided with replacements of the RGS contact residues (46). Moreover, none of the mutants with substituted RGS contact residues had notably altered binding to Pγ. A space-filling model shows that despite a large number of neighbors between RGS and Pγ interacting residues in the primary structure of $G\alpha_t$ there is no significant overlap between the two surfaces (Fig. 7*B*). This finding is in noteworthy agreement with the similar conclusion made based on the $G\alpha_s$/effector crystal structure (28).

A more detailed mapping on effector surfaces of $G\alpha_t$ than biochemical tools can provide is to be attained from a crystal structure of transducin complexed with Pγ or holoPDE. The potential for simultaneous binding of effector and RGS proteins to Gα subunits brings up an intriguing possibility of a new interface between RGS and Gα effector. Trimeric complexes between Gα subunits, their effectors, and RGS proteins may play an important role in rapid termination of G protein-mediated signals.

Acknowledgments—We thank R. McEntaffer for technical assistance and Drs. H. Hamm and N. Skiba for the $G\alpha_t/G\alpha_{i1}$ expression vector.

REFERENCES

1. Chabre, M., and Deterre, P. (1989) *Eur. J. Biochem.* **179,** 255–266
2. Yarfitz, S., and Hurley, J. B. (1994) *J. Biol. Chem.* **269,** 14329–14332
3. Stryer, L. (1996) *Proc. Natl. Acad. Sci. U. S. A.* **93,** 557–559
4. Dohlman, H. G., and Thorner, J. (1997) *J. Biol. Chem.* **272,** 3871–3874
5. Koelle, M. R. (1997) *Curr. Opin. Cell Biol.* **9,** 143–147
6. Berman, D. M., and Gilman, A. G. (1998*) J. Biol. Chem.* **273,** 1269–1272
7. He, W., Cowan, C. W., and Wensel, T. G. (1998) *Neuron* **20,** 95–102
8. Chen, C. K., Wieland, T., and Simon, M. I. (1996) *Proc. Natl. Acad. Sci. U. S. A.* **93,** 12885–12889
9. Faurobert, E., and Hurley, J. B. (1997) *Proc. Natl. Acad. Sci. U. S. A.* **94,** 2945–2950
10. Berman, D. M., Kozasa, T., and Gilman, A. G. (1996) *J. Biol. Chem.* **271,** 27209–27212
11. Natochin, M., Granovsky, A. E., and Artemyev, N. O. (1997) *J. Biol. Chem.* **272,** 17444–17449
12. Noel, J. P., Hamm, H. E., and Sigler, P. B. (1993) *Nature* **366,** 654–663
13. Lambright, D. G., Noel, J. P., Hamm, H. E., and Sigler, P. B. (1994) *Nature* **369,** 621–628
14. Coleman, D. E., Berghuis, A. M., Lee, E., Linder, M. E., Gilman, A. G., and Sprang, S. R.(1994) *Science* **265,** 1405–1412
15. Sondek, J., Lambright, D. G., Noel, J. P., Hamm, H. E., and Sigler, P. B. (1994) *Nature* **372,** 276–279
16. Mixon, M. B, Lee, E., Coleman, D. E., Berghuis, A. M., Gilman, A. G., and Sprang, S. R. (1995) *Science* **270,** 954–960
17. Itoh, H., and Gilman, A. G. (1991) *J. Biol. Chem.* **266,** 16226–16231
18. Berlot, C. H., and Bourne, H. R. (1992) *Cell* **68,** 911–922
19. Rarick, H. M., Artemyev, N. O., and Hamm, H. E. (1992) *Science* **256,** 1031–1033
20. Artemyev, N. O., Rarick, H. M., Mills, J. S., Skiba, N. P., and Hamm, H. E. (1992) *J. Biol. Chem.* **267,** 25067–25072
21. Artemyev, N. O., Mills, J. S., Thornburg, D. R., Knapp, D. R., Schey, K. L., and Hamm, H. E. (1993) *J. Biol. Chem.* **268,** 23611–23615
22. Liu, Y., Arshavsky, V. Y., and Ruoho, A. E. (1996*) J. Biol. Chem.* **271,** 26900–26907
23. Skiba, N. P., Bae, H., and Hamm, H. E. (1996) *J. Biol. Chem.* **271,** 413–424
24. Faurobert, E., Otto-Bruc, A., Chardin, P. and Chabre, M. (1993) *EMBO J.* **12,** 4191–4198
25. Li, Q., and Cerione, R. A. (1997) *J. Biol. Chem.* **272,** 21673–21676
26. Grishina, G., and Berlot, C. H. (1997) *J. Biol. Chem.* **272,** 20619–20626
27. Tesmer, J. J. G., Sunahara, R. K., Gilman, A. G., and Sprang, S. R. (1997) *Science* **278,** 1907–1916
28. Sunahara, R. K., Tesmer, J. J. G., Gilman, A. G., and Sprang, S. R. (1997) *Science* **278,** 1943–1947
29. Papermaster, D. S., and Dreyer, W. J. (1974) *Biochemistry* **13,** 2438–2444
30. Yamanaka, G., Eckstein, F., and Stryer, L. (1985) *Biochemistry* **24,** 8094–8101
31. Yamazaki, A., Tatsumi, M., and Bitensky, M. W. (1988) *Methods Enzymol.* **159,** 702–710
32. Kleuss, C., Pallas, M., Brendel, S., Rosenthal, W., and Schultz, G. (1987) *J. Chromatogr.* **407,** 281–289
33. Artemyev, N. O. (1997) *Biochemistry* **36,** 4188–4193
34. Kleuss, C., Raw, A. S., Lee, E., Sprang, S. R., and Gilman, A. G. (1994) *Proc. Natl. Acad. Sci. U. S. A.* **91,** 9828–9831
35. Arshavsky, V. Y., Gray-Keller, M. P., and Bownds, M. D. (1991) *J. Biol. Chem.* **266,** 18530–18537
36. Artemyev, N. O., and Hamm, H. E. (1992) *Biochem. J.* **283,** 273–279
37. Thompson, W. J., and Appleman, M. M. (1971) *Biochemistry* **10,** 311–316
38. Bradford, M. M. (1976) *Anal. Biochem.* **72,** 248–254
39. Laemmli, U. K. (1970) *Nature* **227,** 680–685
40. Mittal, R., Erickson, J. W. and Cerione, R. A. (1996) *Science* **271,** 1413–1416
41. Natochin, M., and Artemyev, N. O. (1998) *J. Biol. Chem.* **273,** 4300–4303
42. Fung, B. K.-K., and Nash, C. (1983) *J. Biol. Chem.* **258,** 10503–10510
43. Iiri, T., Farfel, Z., and Bourne, H. R. (1997) *Proc. Natl. Acad. Sci. U. S. A.* **94,** 5656–5661
44. Onrust, R., Herzmark, P., Chi, P., Garcia, P. D., Lichtarge, O., Kingsley, C., and Bourne, H. R. (1997) *Science* **275,** 381–384
45. Lambright, D. G., Sondek, J., Bohm, A., Skiba, N. P., Hamm, H. E., and Sigler, P. B. (1996) *Nature* **379,** 311–319
46. Tesmer, J. J. G., Berman, D. M., Gilman, A. G., and Sprang, S. R. (1997) *Cell* **89,** 251–261
47. Chen, C., Zheng, B., Han, J., and Lin, S.-C. (1997) *J. Biol. Chem.* **272,** 8679–8685
48. Hunt, T. W., Fields, T. A., Casey, P. J., and Peralta, E. G. (1996) *Nature* **383,** 175–177
49. Venkatakrishnan, G., and Exton, J. H. (1996) *J. Biol. Chem.* **271,** 5066–5072
50. Spickofsky, N., Robichon, A., Danho, W., Fry, D., Greeley, D., Graves, B., Madison, V., and Margolskee, R. F. (1994) *Nat. Struct. Biol.* **1,** 771–781
51. Berman, D. M., Wilkie, T. M., and Gilman, A. G. (1996) *Cell* **86,** 445–452
52. Watson, N., Linder, M. E., Druey, K. M., Kehrl, J. H., and Blumer, K. J. (1996) *Nature* **383,** 172–175
53. Hepler, J. R., Berman, D. M., Gilman, A. G., and Kozasa, T. (1997) *Proc. Natl. Acad. Sci. U. S. A.* **94,** 428–432
54. Yan, Y., Chi, P. P., and Bourne, H. R. (1997) *J. Biol. Chem.* **272,** 11924–11927

Identification of Effector Residues on Photoreceptor G Protein, Transducin

Michael Natochin, Alexey E. Granovsky and Nikolai O. Artemyev

J. Biol. Chem. 1998, 273:21808-21815.
doi: 10.1074/jbc.273.34.21808